FUTURE TECHNO SCIENCE

Journal of Future Artificial Intelligence and Technologies

E-ISSN: 3048-3719

Research Article

Hourly UV Index Forecasting Across Climatic Zones in Sri Lanka: A Residual-Correction Hybrid Machine Learning and Deep Learning Approach

Hiruni Navodya Kudagama *, Samantha Mathara Arachchi, K. G. Amidu Yohan, and C. L. I. S. Fonseka

University of Colombo School of Computing, University of Colombo, Colombo 00700, Sri Lanka;
e-mail : hiruninkudagama0323@gmail.com; ssp@ucsc.cmb.ac.lk; amiduyohan111@gmail.com; cli@ucsc.cmb.ac.lk

* Corresponding Author : Hiruni Navodya Kudagama

Abstract: Ultraviolet (UV) radiation reaching the Earth's surface has shown a long-term increasing trend, raising concerns due to its adverse effects on human health, including an elevated risk of skin cancer. The Ultraviolet Index (UVI) is a standardized measure of UV radiation intensity and plays an important role in public health protection and climate adaptation planning. However, UVI forecasting studies in Sri Lanka remain limited, particularly those comparing traditional statistical, machine learning (ML), deep learning (DL), and hybrid forecasting approaches across different climatic zones. This study develops and evaluates forecasting frameworks for hourly UVI prediction in three representative climatic regions of Sri Lanka: Colombo (wet zone), Badulla (intermediate zone), and Jaffna (dry zone). Hourly UVI observations from January 2018 to December 2023 were obtained from the NASA POWER database. Since UVI values between 18:00 and 05:00 were consistently zero, the analysis was restricted to daylight hours (06:00–17:00). Traditional time-series, ML, and DL models were evaluated for one-hour-ahead forecasting using a univariate framework. In addition, a residual-correction hybrid approach was proposed, in which residuals from the best-performing standalone model were modeled using a secondary learning algorithm to improve prediction accuracy. The results show that ML and DL models consistently outperform traditional statistical approaches, while hybrid models achieve the highest predictive performance across all climatic zones. The CNN–RF hybrid achieved the best performance in Colombo (RMSE = 0.3967, R^2 = 0.9881), whereas the FNN–RF hybrid performed best in Badulla (RMSE = 0.4265, R^2 = 0.9847) and Jaffna (RMSE = 0.4291, R^2 = 0.9844). Furthermore, lag analysis revealed that both short-term dependencies and recurring diurnal patterns contribute substantially to forecasting performance. These findings demonstrate the effectiveness of residual-correction hybrid forecasting for regional UVI prediction and its potential application in public health early warning systems.

Keywords: Climate adaptation; Deep learning; Environmental forecasting; Machine learning; Public health; Residual-correction hybrid model; Ultraviolet index forecasting; UV radiation.

Received: April, 21st 2026
Revised: June, 16th 2026
Accepted: June, 17th 2026
Published: June, 22nd 2026
Curr. Ver.: June, 22nd 2026

1. Introduction

Ultraviolet (UV) radiation reaching the Earth's surface has shown a long-term increasing trend, posing significant risks to human health through elevated incidences of skin cancer, cataracts, and immune system suppression [1]–[4]. The Ultraviolet Index (UVI), developed by the World Health Organization, is a standardized indicator used to communicate UV radiation intensity and associated health risks to the public [5], [6]. As climate change continues to influence atmospheric composition, ozone concentrations, and cloud-cover dynamics, accurate short-term UVI forecasting has become increasingly important for supporting public health interventions, risk communication, and climate adaptation strategies [4], [7]–[9]. Reliable forecasts can enable proactive measures to reduce harmful UV exposure and strengthen environmental health management, particularly in regions experiencing high solar irradiance throughout the year.

Despite its practical importance, accurate UVI forecasting remains a challenging task. Physical radiative transfer models (RTMs), such as UVSPEC and TUV, provide physically interpretable forecasts but require detailed atmospheric and radiometric inputs that are often unavailable in data-sparse regions [10], [11]. To address these limitations, machine learning (ML) and deep learning (DL) approaches have increasingly been adopted for environmental forecasting applications due to their ability to capture complex nonlinear relationships directly from observational data [12], [13]. Although these approaches have demonstrated promising performance in solar radiation and related environmental prediction tasks, their application to UVI forecasting remains relatively limited, particularly in tropical environments.

Most existing UVI forecasting studies have been conducted in temperate or high-latitude regions, while comparatively little attention has been given to tropical countries characterized by distinct climatic regimes and year-round solar exposure. Furthermore, previous studies have predominantly focused on individual forecasting models, with limited efforts devoted to systematically comparing traditional time-series (TTS), ML, DL, and hybrid approaches under different climatic conditions. Hybrid residual-correction frameworks, which have demonstrated effectiveness in improving forecasting accuracy in other time-series domains, have also received limited attention in the context of UVI prediction. Consequently, the relative strengths of standalone and hybrid forecasting approaches across different tropical climatic zones remain insufficiently understood.

Sri Lanka provides a suitable case study for addressing these research gaps because it comprises three major climatic zones, the Wet Zone, Intermediate Zone, and Dry Zone, which exhibit substantial differences in rainfall patterns, cloud cover, humidity, and solar exposure [14]. To capture this climatic diversity, the present study focuses on three representative districts: Colombo (wet zone), Badulla (intermediate zone), and Jaffna (dry zone). We hypothesize that residual-correction hybrid models can exploit complementary information contained in both primary forecasts and residual error structures, thereby improving predictive performance compared with standalone TTS, ML, and DL models for short-term UVI forecasting.

To investigate this hypothesis, a residual-correction hybrid forecasting framework is developed and evaluated for one-hour-ahead UVI prediction using hourly NASA POWER observations collected between January 2018 and December 2023. The study pursues three objectives:

- To investigate the effectiveness of residual-correction hybrid forecasting for hourly UVI prediction across different climatic zones in Sri Lanka.
- To examine temporal dependency patterns and lag structures that contribute to UVI predictability in wet, intermediate, and dry climatic conditions.
- To provide a systematic comparison of traditional time-series, machine learning, deep learning, and hybrid forecasting approaches under a consistent experimental framework.

By analysing UVI dynamics across climatically distinct regions, this study contributes empirical evidence on the applicability of data-driven forecasting methods for tropical environments and highlights the potential of hybrid forecasting strategies for supporting UV early-warning systems, public health planning, and climate adaptation initiatives. The remainder of this paper is organized as follows. Section 2 reviews the literature on UVI forecasting and ML/DL-based environmental prediction. Section 3 presents the study area, dataset, preprocessing procedures, feature engineering strategy, forecasting models, and the proposed hybrid framework. Section 4 provides exploratory data analysis. Section 5 presents the experimental results, while Section 6 discusses the findings and their implications. Finally, Section 7 concludes the paper and outlines future research directions.

2. Literature Review

This section reviews previous studies on ultraviolet index (UVI) forecasting and related environmental time-series prediction problems. Particular attention is given to physical models, machine learning (ML), deep learning (DL), and hybrid forecasting frameworks that have been applied to short-term environmental forecasting tasks. Rather than presenting studies individually, the review focuses on how different methodological families address key forecasting challenges, including nonlinearity, temporal dependence, data availability, and model generalization. This synthesis is subsequently used to identify research gaps and motivate the methodological framework adopted in the present study.

Accurate UVI forecasting remains a challenging problem due to the complex interactions among atmospheric processes, strong temporal variability, nonlinear relationships, and the limited availability of high-resolution environmental observations in many regions. Existing studies have approached these challenges using a range of physical, statistical, ML, DL, and hybrid methods. While each approach offers distinct advantages, they also involve trade-offs in terms of data requirements, predictive performance, interpretability, and operational applicability. Consequently, understanding the strengths and limitations of these methodological families is essential for identifying suitable forecasting strategies, particularly in data-sparse tropical environments.

2.1. Physical and Satellite-Based Approaches to UV Index Estimation

Early efforts to estimate and forecast surface UV radiation primarily relied on physically based radiative transfer models (RTMs). These models simulate the propagation of solar radiation through the atmosphere by explicitly accounting for key physical drivers, including solar zenith angle, total column ozone, aerosol optical depth, cloud optical properties, and surface albedo. Among the most widely used RTM tools are UVSPEC within the libRadtran package and the Tropospheric Ultraviolet and Visible (TUV) model developed by the National Center for Atmospheric Research (NCAR) [11], [15].

Because RTMs are grounded in atmospheric physics, they provide physically interpretable estimates and have been extensively applied in UV climatology studies and future climate scenario analyses [16]. Their ability to quantify the effects of atmospheric composition and radiative processes makes them valuable for scientific investigations of long-term UV variability. However, operational deployment of RTMs for local short-term forecasting remains challenging because they require comprehensive atmospheric inputs that are often unavailable at the spatial and temporal resolutions needed for real-time applications [10], [11].

These limitations are particularly pronounced in tropical and data-sparse regions, where access to reliable atmospheric observations remains limited. Consequently, there is growing interest in data-driven forecasting approaches that can provide accurate short-term UVI predictions while requiring fewer physical input variables. This shift has motivated the increasing adoption of ML and DL techniques for environmental forecasting applications.

2.2. Machine Learning and Deep Learning for UVI Forecasting

Recent advances in ML and DL have created new opportunities for UVI forecasting by enabling the direct learning of complex temporal and nonlinear relationships from historical observations. Compared with physically based approaches, these methods typically require fewer atmospheric inputs and can be adapted more easily to operational forecasting settings. As a result, ML and DL models have increasingly been investigated as alternatives to traditional physical models for short-term UVI prediction.

Several studies have demonstrated the potential of deep learning architectures for UVI forecasting. D et al. [17] employed Gated Recurrent Unit (GRU) networks for short-term UVI prediction in Bengaluru, India, and reported improved forecasting performance when temporal variables such as hour of day and day of year were incorporated into the model. While the study demonstrated the effectiveness of recurrent neural networks for capturing temporal patterns, the evaluation was limited to a relatively narrow range of forecasting algorithms and relied on a discretized UVI representation that excluded extreme UV conditions.

A more comprehensive multivariate forecasting framework was proposed by Prasad et al. [18], who developed an Enhanced Joint Hybrid Explainable Deep Neural Network (EJH-X-DNN) for one-hour-ahead UVI prediction across multiple locations in Australia. By integrating satellite-derived variables, ground-based measurements, and explainability mechanisms, the framework achieved superior performance relative to several benchmark models. Nevertheless, the approach depends on a rich set of atmospheric and meteorological predictors, which may not be consistently available in data-sparse environments.

Hybrid deep learning approaches have also demonstrated strong potential for UVI forecasting. Ahmed et al. [19] proposed a CEEMDAN-CLSTM framework that combined signal decomposition techniques with deep learning for daily maximum UVI prediction. Their results highlighted the benefits of integrating decomposition methods and neural networks to capture complex nonlinear temporal dynamics. However, the study focused on daily forecasting rather than short-term hourly prediction, leaving uncertainty regarding the effectiveness of similar architectures for operational one-hour-ahead forecasting tasks.

Beyond regression-based forecasting, ML techniques have also been applied to UVI classification and prediction-related tasks. Syahab et al. [20] used logistic regression and random forest models to classify extreme and non-extreme UVI conditions, demonstrating the superior performance of ensemble learning methods. Similarly, Ervianto et al. [21] compared several ML algorithms, including support vector machines, artificial neural networks, decision trees, and Naïve Bayes classifiers, for estimating UVI from UV-A and UV-B measurements, with support vector machines achieving the highest predictive accuracy. Although these studies confirm the usefulness of ML for UVI-related applications, they focus primarily on classification or measurement estimation rather than the one-hour-ahead forecasting problem considered in the present work.

Collectively, the existing literature demonstrates that ML, DL, and hybrid architectures can substantially improve UVI prediction accuracy compared with traditional approaches. Nevertheless, most studies have been conducted in temperate, arid, or high-latitude environments, and relatively few have investigated forecasting performance across climatically distinct tropical regions. Furthermore, systematic comparisons among traditional time-series, ML, DL, and hybrid forecasting frameworks remain limited, particularly for hourly UVI prediction. These limitations motivate the need for a more comprehensive evaluation framework capable of assessing forecasting performance across multiple climatic conditions and methodological paradigms.

2.3. ML and DL for Meteorological Variable Forecasting

The methodological motivation for this study is further supported by advances in ML and DL-based forecasting of related atmospheric and environmental variables. Although variables such as solar irradiance, photovoltaic power output, and wind speed differ from UVI in their physical interpretation, they share several forecasting characteristics, including strong temporal dependence, nonlinear dynamics, seasonality, and sensitivity to atmospheric conditions. Consequently, methodological developments in these domains provide valuable insights for UVI forecasting.

In solar irradiance forecasting, hybrid deep learning architectures have consistently demonstrated superior performance compared with standalone models. Zang et al. [22] proposed a CNN-LSTM framework for short-term global horizontal irradiance (GHI) forecasting that effectively exploited spatial and temporal dependencies, outperforming standalone CNN and LSTM models across one-hour-ahead forecasting horizons. Similarly, Zhang et al. [23] developed a hybrid forecasting framework incorporating an error-correction stage for photovoltaic power prediction and reported substantial reductions in prediction error relative to standalone deep learning models. These findings suggest that residual information often contains additional predictive patterns that remain unexploited by primary forecasting models.

Recent studies have also highlighted the benefits of integrating feature engineering and model optimization strategies within forecasting frameworks. Taha et al. [24] combined feature selection techniques with advanced ML algorithms for solar irradiance forecasting using NASA POWER data and achieved highly accurate predictions across multiple forecasting horizons. Their work demonstrates the importance of selecting informative predictors and systematically evaluating competing forecasting models within a unified experimental framework. Similar observations have been reported in wind speed forecasting. Taha et al. [25] integrated Variational Mode Decomposition (VMD) with several advanced ML algorithms, including XGBoost, AdaBoost, LightGBM, KNN, and Informer-based architectures, for long-term wind speed prediction. Their results showed that decomposition-based frameworks effectively addressed the non-stationary characteristics of atmospheric time series and significantly improved forecasting performance. Such findings reinforce the broader applicability of hybrid forecasting strategies across environmental prediction problems.

Although solar irradiance, wind speed, and UVI represent distinct environmental variables, they exhibit similar forecasting challenges arising from nonlinear behavior, temporal dependence, seasonality, and atmospheric variability. Consequently, forecasting architectures that have demonstrated success in these related domains, including deep learning, decomposition-based methods, and hybrid residual-correction frameworks, provide a strong methodological foundation for UVI forecasting. The success of these approaches in related environmental forecasting tasks motivates their evaluation for short-term UVI prediction in climatically diverse tropical environments.

2.4. Hybrid Residual-Correction Frameworks in Environmental Forecasting

Among recent developments in environmental forecasting, hybrid modeling strategies have attracted considerable attention because they combine the complementary strengths of multiple algorithms. Rather than relying on a single forecasting model, hybrid approaches seek to capture different aspects of the underlying data-generating process, often leading to improved predictive accuracy and robustness. One particularly effective strategy is residual-correction forecasting, in which the residual errors produced by a primary model are treated as a secondary forecasting target and subsequently modeled using an additional learning algorithm [23]. This approach is especially useful when the primary model successfully captures dominant temporal patterns but leaves structured prediction errors that still contain exploitable information. By learning these residual patterns, the secondary model can refine the initial forecast and reduce systematic prediction errors.

Residual-correction frameworks have been successfully applied in several environmental forecasting domains, including solar irradiance prediction, photovoltaic power forecasting, and UV-related applications [19], [23], [24]. These studies consistently report improvements in forecasting accuracy compared with standalone approaches, highlighting the potential of hybridization for modeling complex nonlinear environmental processes. The effectiveness of these frameworks is often attributed to their ability to combine the strengths of different modeling paradigms while mitigating individual model limitations. The relevance of residual-correction forecasting to UVI prediction is supported by the fact that UVI time series exhibit many of the characteristics observed in solar irradiance and photovoltaic power data, including periodic behavior, nonlinear dynamics, short-term fluctuations, and sensitivity to atmospheric conditions. Consequently, forecasting methodologies that have proven successful in related environmental domains provide a strong theoretical basis for investigating hybrid residual-correction frameworks for short-term UVI prediction.

Despite these promising developments, the application of residual-correction hybridization to hourly UVI forecasting remains limited. Existing hybrid UVI studies have primarily focused on multivariate forecasting settings or daily prediction horizons [18], [19]. Moreover, little attention has been given to systematically combining standalone ML and DL models through residual-correction mechanisms for one-hour-ahead univariate UVI forecasting. This gap provides a clear opportunity for further investigation.

2.5. Research Gaps and Positioning of This Study

The reviewed literature reveals several important gaps that motivate the present research. First, most UVI forecasting studies have been conducted in temperate, arid, or high-latitude regions, including Australia, India, Indonesia, and the Middle East [17]–[21]. Comparatively little evidence is available from tropical island environments such as Sri Lanka, where climatic variability, solar exposure, and atmospheric conditions differ substantially from those reported in existing studies.

Second, although ML, DL, and hybrid forecasting approaches have demonstrated promising performance in both UVI forecasting and related environmental prediction tasks, residual-correction hybridization remains largely unexplored for one-hour-ahead univariate UVI forecasting. Existing hybrid studies have primarily emphasized deep learning architectures, decomposition techniques, or multivariate forecasting frameworks, leaving the potential benefits of residual-correction strategies insufficiently investigated [18], [19], [23].

Third, few studies have conducted a systematic comparison of traditional time-series (TTS), ML, DL, and hybrid forecasting approaches within a unified experimental framework. As a result, the relative strengths and limitations of these methodological families remain difficult to assess, particularly when forecasting performance is evaluated across distinct climatic conditions.

To address these gaps, the present study develops and evaluates a residual-correction hybrid forecasting framework for one-hour-ahead UVI prediction using hourly NASA

POWER observations from three representative climatic zones in Sri Lanka. By combining a systematic comparison of TTS, ML, DL, and hybrid approaches with an analysis of temporal dependency patterns and lag structures, the study provides new empirical evidence on the applicability of data-driven forecasting methods for tropical UVI prediction and offers practical insights for the development of UV early-warning systems.

3. Data and Methodology

This section describes the dataset, preprocessing procedures, feature engineering strategy, and forecasting framework employed for hourly ultraviolet index (UVI) prediction. The workflow includes data acquisition, missing-value treatment, lag-based feature selection, model development, hyperparameter optimization, and performance evaluation. Forecasting performance was assessed using traditional time-series (TTS), machine learning (ML), deep learning (DL), and residual-correction hybrid models under a unified experimental framework to ensure consistent comparison across climatic zones.

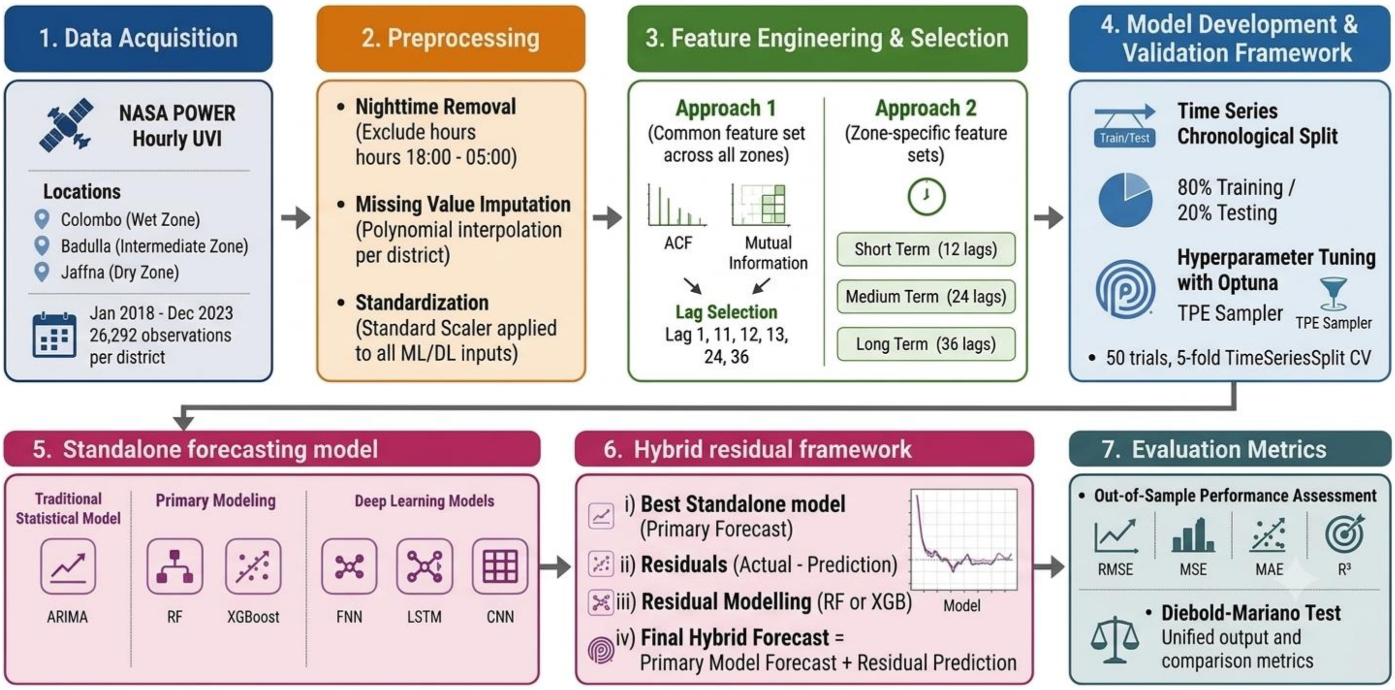

Figure 1. Overall methodological framework of the proposed UVI forecasting system

Figure 1 illustrates the complete methodological workflow adopted in this study. The framework consists of six main stages: data acquisition, preprocessing and missing-value imputation, lag-based feature engineering, model training and hyperparameter optimization, residual-correction hybrid forecasting, and performance evaluation. This structured pipeline enables a systematic comparison of standalone and hybrid forecasting approaches for one-hour-ahead UVI prediction.

3.1. Dataset

Hourly UVI observations covering the period from 1 January 2018 (00:00) to 31 December 2023 (23:00) were obtained from the NASA POWER Data Access Viewer for three representative districts in Sri Lanka: Colombo (6.9271°N, 79.8612°E), Badulla (6.9934°N, 81.0550°E), and Jaffna (9.6615°N, 80.0255°E). These districts were selected to represent the country's major climatic zones, namely the wet, intermediate, and dry zones, respectively. The dataset is derived from the CERES SYN1deg product, which provides satellite-based all-sky estimates of surface ultraviolet radiation. UVI values are calculated within the NASA POWER framework using standard conversion procedures based on surface ultraviolet irradiance measurements (W $m^{-2} \times 40$) [26]–[29]. Data were retrieved using the exact geographic coordinates of each district and exported as comma-separated value (CSV) files for subsequent analysis.

Because ultraviolet radiation is absent during nighttime hours, observations recorded between 18:00 and 05:00 consistently exhibited UVI values equal to zero and therefore provided limited predictive information. To focus the analysis on periods with meaningful solar exposure, only daylight observations between 06:00 and 17:00 were retained. After removing nighttime records, each district contained 26,292 hourly observations, which served as the basis for feature engineering, model training, and forecasting evaluation.

3.2. Missing Value Imputation

Missing observations in the NASA POWER dataset were originally encoded as −999 and were handled using a structured district-specific imputation procedure. Because missing values can introduce bias into time-series forecasting models and distort temporal dependency structures, an objective evaluation process was performed to identify the most appropriate imputation method for each district.

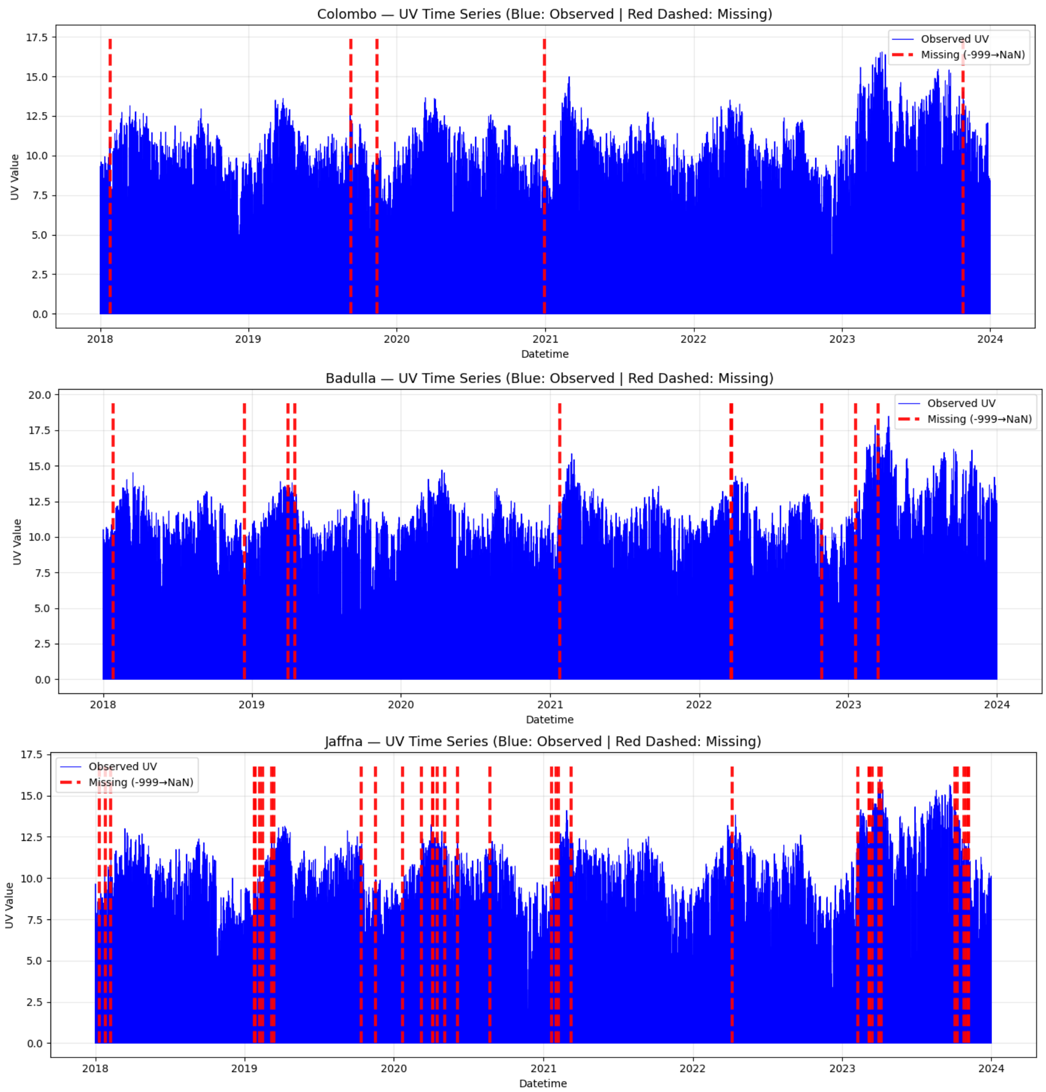

Figure 2. Time-series plots of hourly UVI data with missing observations for Colombo, Badulla, and Jaffna

Figure 2 illustrates the temporal distribution of missing observations across the three districts. To evaluate imputation performance, 5% of complete observations were randomly removed from continuous data segments following established validation procedures for time-series imputation studies [30], [31]. Several univariate imputation techniques were then applied, including linear interpolation, forward filling, backward filling, Kalman filtering, polynomial interpolation (orders 2–5), and spline interpolation (orders 2–5).

The resulting imputations were evaluated using RMSE, MSE, MAE, and R^2. The best-performing method for each district was selected according to overall reconstruction accuracy. As summarized in Table 1, third-order polynomial interpolation produced the most accurate results for Colombo, whereas second-order polynomial interpolation yielded the best performance for both Badulla and Jaffna.

Table 1. Summary of missing values and selected imputation methods

District	Missing Values (%)	Evaluation Subset	Selected Imputation Method
Colombo	0.0057	15 Apr 2019 10:00 – 29 Aug 2022 07:00	Polynomial Interpolation (Order 3)
Badulla	0.0076	14 Nov 2019 09:00 – 05 Feb 2022 09:00	Polynomial Interpolation (Order 2)
Jaffna	0.0399	05 Jun 2020 10:00 – 14 May 2022 10:00	Polynomial Interpolation (Order 2)

The relatively low proportion of missing observations across all districts indicates high overall data completeness. Nevertheless, performing a systematic imputation assessment was necessary to preserve temporal continuity and ensure reliable downstream forecasting performance.

3.3. Feature Selection Using Autocorrelation and Mutual Information Analysis

Effective lag selection is critical for time-series forecasting because predictive performance depends strongly on the ability of input features to capture temporal dependencies. To identify informative lag structures for one-hour-ahead UVI forecasting, a combination of autocorrelation analysis and mutual information (MI) analysis was employed. The autocorrelation function (ACF) was first used to identify dominant linear temporal dependencies within the hourly UVI series. Because UVI dynamics may also contain nonlinear relationships that cannot be fully captured by correlation-based measures, MI analysis was subsequently applied to lag values extending up to 72 hours (three days). While ACF measures linear dependence, MI quantifies both linear and nonlinear associations between lagged observations and the forecasting target, thereby providing a more comprehensive assessment of feature relevance.

Candidate lag features were initially identified from the ACF and MI profiles, after which elbow points in the MI curves were used to refine the search space. A Random Forest model was then trained using progressively larger lag subsets, and forecasting errors were evaluated to determine the point at which additional lag variables no longer produced meaningful performance improvements. This procedure was applied consistently across all districts to ensure a comparable feature engineering process.

The results of both ACF and MI analyses revealed highly consistent temporal dependency patterns across the three climatic zones. In particular, strong predictive information was observed for the immediately preceding hour (lag 1), neighboring hours around the same time on the previous day (lags 11, 12, and 13), and the same hour two and three days earlier (lags 24 and 36). These lag structures reflect the strong diurnal and multi-day periodicity of solar radiation processes and indicate that hourly UVI dynamics are influenced by both short-term persistence and recurring daily cycles. The selected lag features were subsequently used as inputs for all forecasting models evaluated in this study.

3.4. Time-Series Validation Framework

To preserve temporal ordering and avoid information leakage, a time-series validation strategy was adopted throughout model development. The dataset was chronologically divided into training (80%) and testing (20%) subsets, with the most recent observations reserved for out-of-sample evaluation. Within the training set, hyperparameter optimization was performed using a five-fold TimeSeriesSplit cross-validation scheme (N_SPLITS = 5), ensuring that each training fold chronologically preceded its corresponding validation fold.

This validation strategy more closely reflects real-world forecasting conditions, where future observations are unavailable during model training.

For ML and DL models, hyperparameter optimization was conducted using the Optuna framework with a Tree-structured Parzen Estimator (TPE) sampler. A total of 50 optimization trials (N_TRIALS = 50) were performed for each model, with mean squared error (MSE) used as the optimization objective. To improve reproducibility, fixed random seeds were applied whenever supported by the underlying algorithms and software libraries. Following hyperparameter optimization, the final model was retrained using the complete training dataset and subsequently evaluated on the independent hold-out test set. This procedure provides an unbiased assessment of forecasting performance on unseen future observations.

3.5. Forecasting Models

The forecasting task considered in this study is one-hour-ahead UV index prediction, formulated as a univariate time-series regression problem. To ensure a fair comparison, all forecasting models were trained using the same lag-based feature representation derived from the feature engineering stage. The evaluated models span four methodological categories: traditional statistical time-series models, machine learning models, deep learning models, and residual-correction hybrid models.

For ML and DL models, hyperparameter optimization was performed using Optuna and the validation framework described in Section 3.4. The corresponding hyperparameter search spaces are summarized in Table 2. The selected model portfolio was designed to represent different forecasting paradigms, ranging from linear statistical approaches to nonlinear ensemble learning and neural-network-based architectures, thereby enabling a comprehensive evaluation of forecasting performance across distinct climatic zones.

Table 2. Hyperparameter search spaces used for model optimization

Model	Hyperparameter	Search Space
RF	n_estimators	{50, 100, 150}
	max_depth	{None, 10, 20}
	min_samples_split	[2, 6]
	min_samples_leaf	[1, 4]
	max_features	{sqrt, log2}
XGBoost	n_estimators	{50, 100, 150, 200}
	max_depth	[3, 9]
	learning_rate	[0.01, 0.3] (log scale)
	subsample	[0.6, 1.0]
	min_child_weight	[1, 5]
FNN	n_layers	{1, 2}
	hidden_units_per_layer	{32, 64, 96, 128}
	activation	{ReLU, tanh}
	L2 regularization (α)	[1×10^{-4}, 1×10^{-2}] (log scale)
LSTM	units	{20, 40, 60, 80}
	dropout_rate	[0.1, 0.4]
	learning_rate	[1×10^{-4}, 1×10^{-2}] (log scale)
	batch_size	{32, 64}
	epochs	{20, 30, 40, 50}
CNN	filters	{32, 64, 96}
	kernel_size	[1, 3]
	learning_rate	[1×10^{-4}, 1×10^{-2}] (log scale)
	batch_size	{16, 32}
	epochs	{10, 20, 30}

The selected search ranges were chosen to balance optimization effectiveness and computational feasibility while covering commonly used parameter values reported in previous forecasting studies.

3.5.1. Traditional Statistical Model

An Autoregressive Integrated Moving Average (ARIMA) model was included as a statistical baseline for comparison. ARIMA is widely used for modeling linear temporal dependencies in time-series data and provides a useful reference against which more complex nonlinear forecasting approaches can be evaluated. The optimal model configuration (p, d, q) was automatically determined using the auto_arima procedure based on minimization of the Akaike Information Criterion (AIC).

3.5.2. Machine Learning Models

Two ensemble-based ML models were evaluated: Random Forest (RF) and Extreme Gradient Boosting (XGBoost). These algorithms were selected because of their ability to model nonlinear relationships, handle feature interactions effectively, and perform well in structured tabular forecasting problems. RF improves generalization through bootstrap aggregation, whereas XGBoost employs gradient boosting and regularization mechanisms to iteratively reduce prediction errors.

3.5.3. Deep Learning Models

Three DL architectures were considered: Feedforward Neural Networks (FNN), Long Short-Term Memory (LSTM) networks, and one-dimensional Convolutional Neural Networks (CNNs). The FNN serves as a nonlinear regression baseline operating on lag-engineered features. LSTM was included because of its capability to model temporal dependencies through gated memory mechanisms, while CNN was employed to capture local patterns and interactions among adjacent lag features.

In this study, temporal information was represented through lag-based feature engineering rather than long sequential input windows. Consequently, the LSTM architecture operated on lag-engineered inputs with a timestep dimension of one, ensuring consistency across all forecasting models and enabling a controlled comparison of forecasting paradigms. Similarly, the CNN architecture was designed to learn localized relationships among neighboring lag features, which are known to play an important role in short-term UVI dynamics.

4. Exploratory Data Analysis

This section presents an exploratory data analysis (EDA) of the ultraviolet index (UVI) series to characterize temporal variability, seasonal behavior, and regional exposure patterns prior to model development. Understanding these characteristics is important for selecting appropriate forecasting features and interpreting model performance across different climatic zones. Time-series visualizations were therefore examined to identify recurring patterns, long-term trends, and periods associated with elevated UV exposure.

4.1. Temporal Variations in Daily Average UVI

Figure 3 illustrates the seasonal variation in daily average UVI across the three study districts. A clear and recurring annual pattern can be observed in all locations, with higher UVI values generally occurring during the early months of the year, followed by a relatively stable period and a gradual decline toward the end of the year. Despite differences in climatic conditions among the districts, the overall temporal behavior remains broadly consistent, reflecting the strong influence of seasonal solar radiation cycles on surface UV exposure.

A notable observation is the consistently elevated UVI levels recorded during 2023 compared with previous years. This pattern is evident across all districts and throughout much of the annual cycle, suggesting a recent increase in UV exposure intensity. The persistence of this pattern across geographically distinct climatic zones indicates that the observed increase is unlikely to be driven solely by local variability and may warrant further investigation in future climatological studies.

4.2. Temporal Variations in Monthly Average UVI

The monthly aggregation of UVI values provides further evidence of increasing UV exposure over the study period. As shown in Figure 4, the monthly average UVI recorded during 2023 remained consistently higher than corresponding monthly values observed in previous years. This pattern is visible across multiple months rather than being restricted to isolated peak periods, suggesting a broader upward shift in UVI intensity.

The observed increase in monthly average UVI is consistent with the daily-scale patterns discussed in the previous subsection. Although the present study focuses on forecasting rather than climatological attribution, these findings highlight the importance of continuous UV monitoring and reinforce the need for reliable forecasting systems capable of supporting public health risk communication and adaptive mitigation strategies.

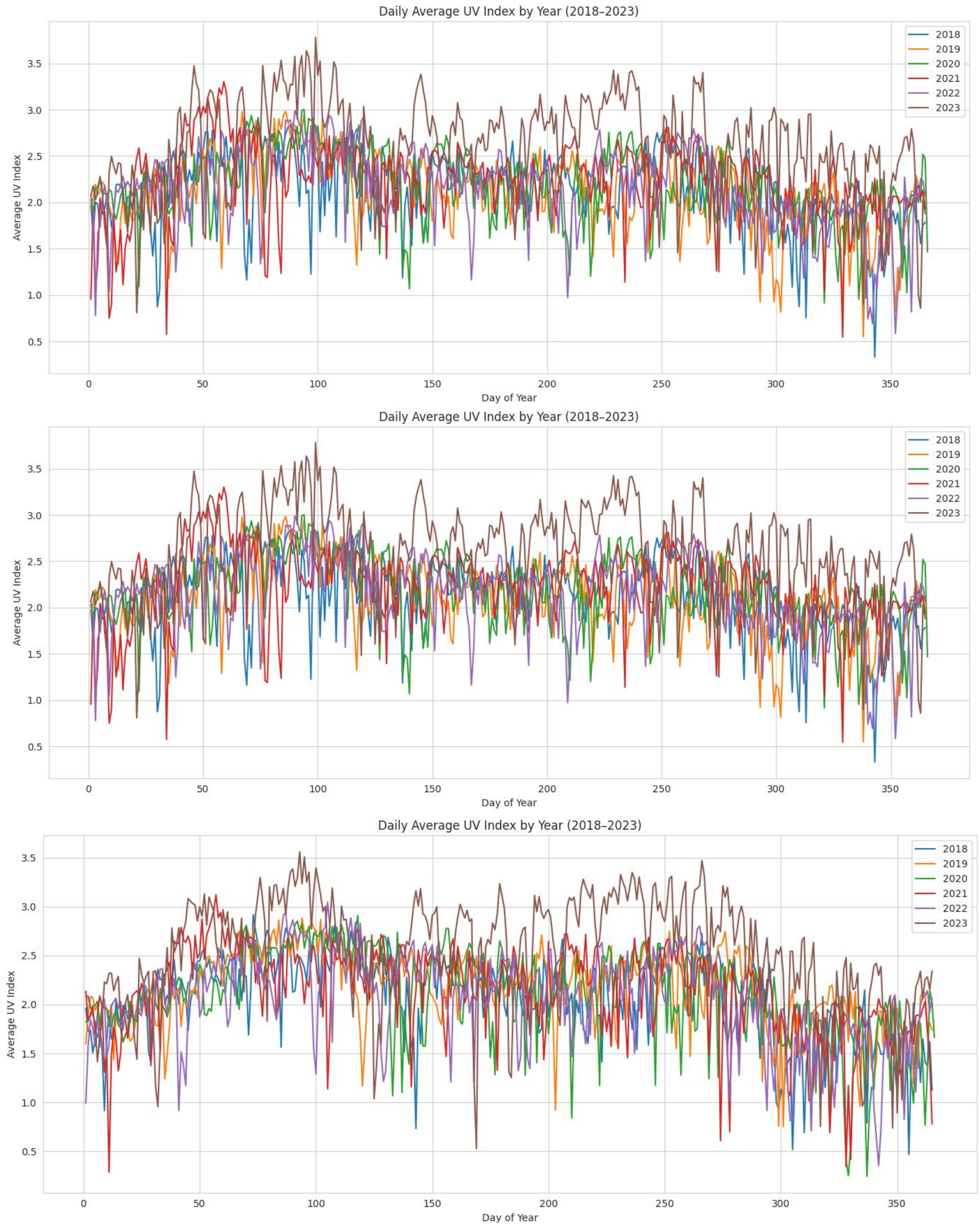

Figure 3. Seasonal plots of daily average UVI for Colombo, Badulla, and Jaffna

4.3. Regional Exposure Patterns of UVI Risk Levels

The World Health Organization (WHO) and the World Meteorological Organization (WMO) classify UVI exposure into five risk categories: Low (0–2), Moderate (3–5), High (6–7), Very High (8–10), and Extreme (≥11) [9], [17], [32], [33]. These categories provide a standardized framework for assessing potential health risks associated with UV exposure and are widely used in public health communication.

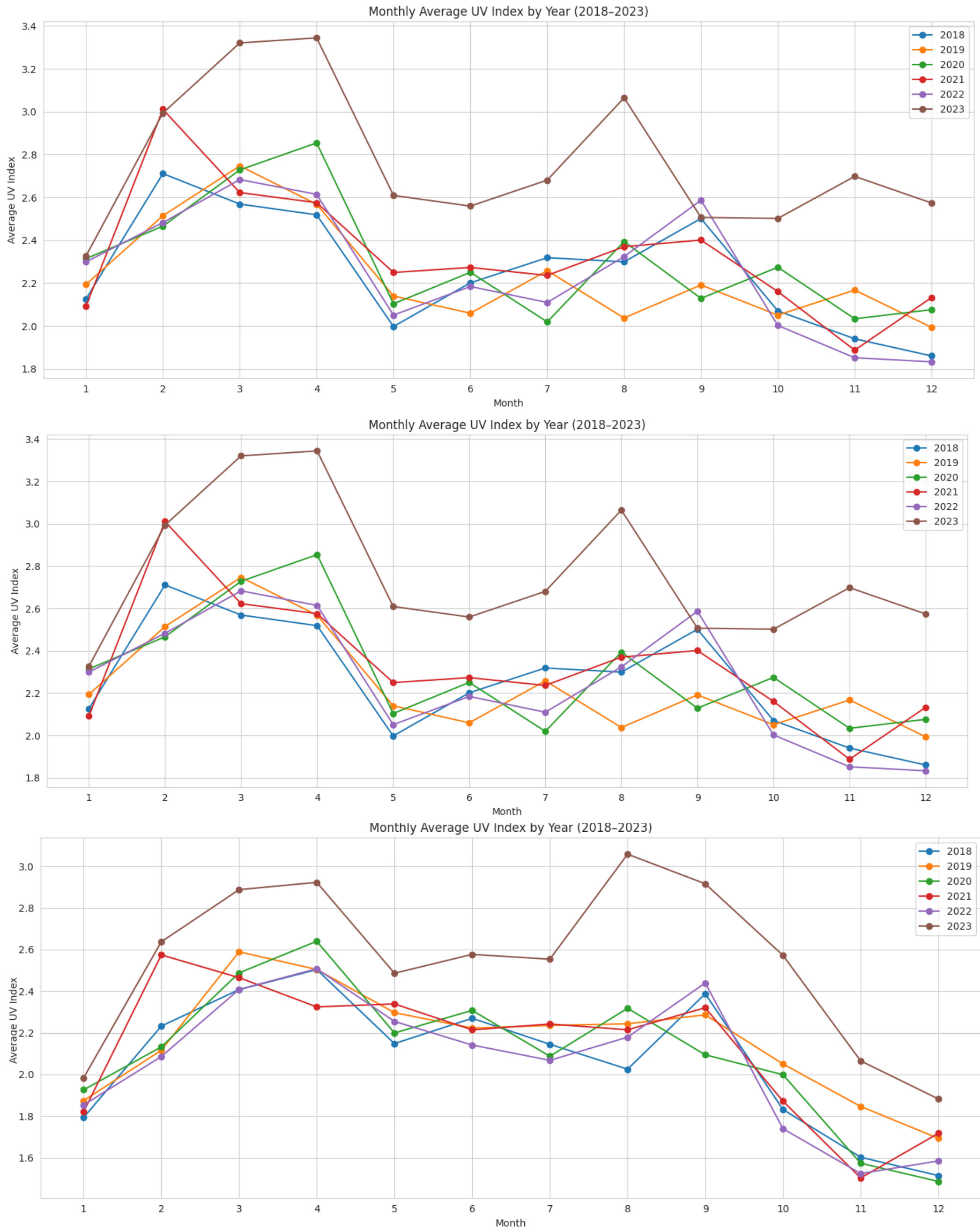

Figure 4. Seasonal plots of monthly average UVI for Colombo, Badulla, and Jaffna

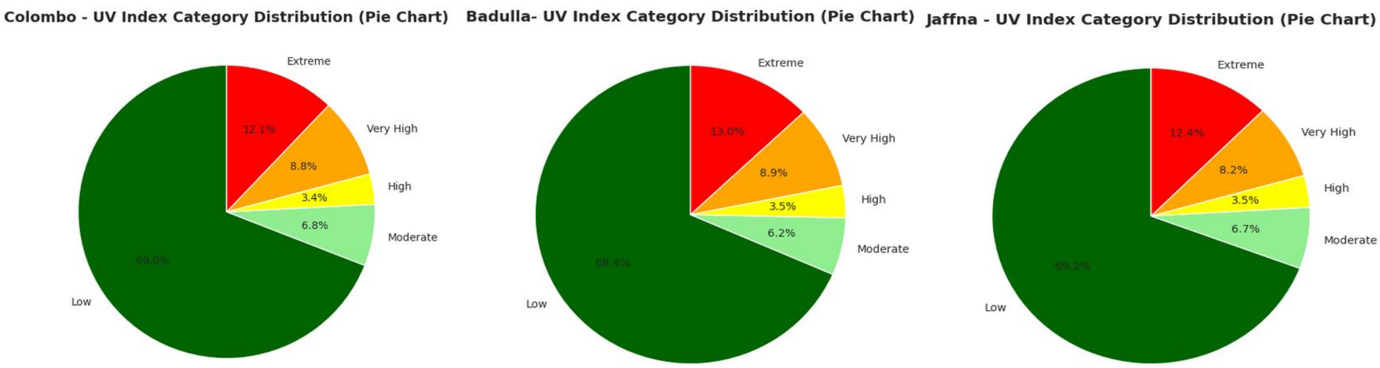

Figure 5. Proportion of high-risk UVI levels across districts

Figure 5 summarizes the distribution of high-risk UVI categories across the three districts. Among the study locations, Badulla recorded the highest combined proportion of High, Very High, and Extreme UVI conditions, accounting for 25.4% of all observations. Colombo and Jaffna also exhibited substantial exposure levels, with corresponding proportions of 24.3% and 24.1%, respectively. Although the differences among districts are relatively modest, the results indicate that elevated UV exposure is a common characteristic across all climatic zones considered in this study. These findings demonstrate that populations in all three regions are regularly exposed to potentially harmful UV conditions. Consequently, accurate short-term UVI forecasting may provide valuable support for UV early-warning systems, public health advisories, and risk mitigation efforts aimed at reducing exposure-related health impacts.

5. Experiments and Results

This section presents the forecasting performance of the evaluated models across the three climatic zones. The results are organized into three stages: (i) benchmarking using a traditional statistical model, (ii) evaluation of standalone ML and DL models, and (iii) assessment of different lag-window strategies for capturing short-, medium-, and long-term temporal dependencies.

5.1. Benchmarking with Traditional Time-Series Models

The Autoregressive Integrated Moving Average (ARIMA) model was employed as the traditional statistical benchmark for one-hour-ahead UVI forecasting. Model configurations were automatically selected using the auto_arima procedure based on minimization of the Akaike Information Criterion (AIC). Table 3 summarizes the performance of the optimized ARIMA models across the three districts.

Table 3. Performance of ARIMA models across climatic zones

District	Model	RMSE	MSE	MAE
Colombo	ARIMA(5,0,4)	3.9644	15.7164	2.1418
Badulla	ARIMA(4,0,2)	3.1761	10.0879	2.6542
Jaffna	ARIMA(4,0,5)	3.1307	9.8010	2.5895

The ARIMA models exhibited substantially larger prediction errors than the ML and DL models evaluated subsequently, indicating limited capability in capturing the nonlinear and recurring temporal patterns present in hourly UVI data. These results highlight the need for more flexible forecasting approaches capable of modelling complex dependencies beyond linear autoregressive relationships.

5.2. Performance of Standalone Forecasting Models

Building upon the lag structures identified through autocorrelation and mutual information analyses, several standalone forecasting models were evaluated, including Random Forest (RF), XGBoost, Feedforward Neural Networks (FNN), Long Short-Term Memory (LSTM), and one-dimensional Convolutional Neural Networks (CNN). All models were trained and evaluated using the validation framework described in Section 3.

Table 4 shows that all ML and DL models substantially outperformed the ARIMA benchmark across the three districts. For Colombo, the CNN model achieved the best overall performance with an RMSE of 0.4519 and an R^2 of 0.9845. In contrast, FNN produced the strongest results in both Badulla and Jaffna, achieving RMSE values of 0.4868 and 0.4868, respectively, together with the highest coefficients of determination (R^2 = 0.9801).

Ensemble learning models, particularly RF and XGBoost, consistently delivered competitive performance across all climatic zones, demonstrating their ability to capture nonlinear relationships within the lag-engineered feature space. Although LSTM is specifically designed for temporal modelling, its performance was generally inferior to FNN and CNN in this study. This outcome suggests that, when temporal information is explicitly encoded through lag-based feature engineering, simpler neural architectures may be sufficient to model short-term UVI dynamics effectively.

Table 4. Performance of ML and DL models using the fixed-lag feature set

Model	MSE	RMSE	MAE	R^2
Colombo				
Random Forest	0.2244	0.4737	0.2579	0.9830
XGBoost	0.2234	0.4726	0.2652	0.9831
FNN	0.2114	0.4598	0.2560	0.9840
LSTM	0.2409	0.4908	0.2898	0.9817
CNN (1-D)	**0.2042**	**0.4519**	**0.2566**	**0.9845**
Badulla				
Random Forest	0.2779	0.5271	0.2853	0.9767
XGBoost	0.2732	0.5226	0.2936	0.9771
FNN	**0.2370**	**0.4868**	**0.2765**	**0.9801**
LSTM	0.3247	0.5698	0.3657	0.9728
CNN (1-D)	0.2559	0.5058	0.3121	0.9785
Jaffna				
Random Forest	0.2779	0.5271	0.2853	0.9767
XGBoost	0.2732	0.5226	0.2936	0.9771
FNN	**0.2370**	**0.4868**	**0.2765**	**0.9801**
LSTM	0.2685	0.5182	0.3163	0.9775
CNN (1-D)	0.2652	0.5150	0.3072	0.9778

5.3. Impact of Lag-Window Length on Forecasting Performance

To investigate the influence of temporal context on forecasting accuracy, additional experiments were conducted using progressively larger lag windows representing short-term (12 lags), medium-term (24 lags), and long-term (36 lags) dependencies. These lag windows approximately correspond to one, two, and three days of historical observations, respectively.

The results presented in Table 5 indicate that forecasting performance is sensitive to the amount of temporal information included in the input feature set. Across the three districts, medium- and long-term lag windows generally produced lower prediction errors than the shorter 12-lag configuration, indicating that UVI forecasting benefits from incorporating information beyond the immediately preceding day.

For Colombo, the best performance was achieved by the CNN model using the 36-lag configuration (RMSE = 0.4107, R^2 = 0.9872). In contrast, FNN achieved the highest accuracy in both Badulla and Jaffna under the 36-lag setting, with RMSE values of 0.4387 and 0.4387, respectively, and R^2 values approaching 0.984. These findings are consistent with the lag-selection analysis presented in Section 3.3, which identified recurring dependencies associated with daily and multi-day solar radiation cycles.

A comparison between Tables 4 and 5 further demonstrates that the varying-lag strategy consistently improved forecasting accuracy relative to the fixed-lag approach. This observation suggests that incorporating broader temporal contexts enables the models to better capture periodic and persistent patterns in UVI dynamics, thereby enhancing predictive performance across different climatic zones.

5.4. Optimal Standalone Model Selection

The forecasting results presented in Table 5 indicate that the optimal standalone model varied across the three climatic zones, reflecting differences in local UVI dynamics and temporal dependency structures. Following hyperparameter optimization using Optuna and TimeSeriesSplit cross-validation, the best-performing model for each district was selected based on forecasting accuracy on the independent test set. The CNN model achieved the best performance for Colombo, whereas the FNN model emerged as the optimal predictor for both Badulla and Jaffna. Notably, all selected models were associated with the 36-lag configuration, suggesting that information from multiple preceding days consistently improved forecasting performance and highlighting the importance of medium- and long-term temporal dependencies in hourly UVI prediction. The optimized hyperparameter configurations reported in Table 6 were subsequently used as the forecasting models in the hybrid residual-correction framework described in the following section.

Table 5. Forecasting performance using different lag-window configurations

District	Window	N_{Lags}	Model	MSE	RMSE	MAE	R²
Colombo	Short-term - One Day (12 lags)	12	RF	0.183513	0.428384	0.239184	0.986081
		12	XGB	0.185133	0.430271	0.246514	0.985958
		12	FNN	0.175221	0.418594	0.251408	0.986710
		12	LSTM	0.208101	0.456180	0.295365	0.984216
		12	CNN	0.197829	0.444779	0.269871	0.984995
	Medium-term - Two Day (24 lags)	24	RF	0.209284	0.457475	0.254811	0.984127
		24	XGB	0.186309	0.431635	0.243076	0.985869
		24	FNN	0.169546	0.411759	0.238763	0.987141
		24	LSTM	0.187634	0.433167	0.275289	0.985769
		24	CNN	0.169668	0.411908	0.235663	0.987131
	Long-term - Three Day (36 lags)	36	RF	0.223180	0.472420	0.260395	0.983077
		36	XGB	0.186064	0.431351	0.242311	0.985892
		36	FNN	0.171764	0.414445	0.246994	0.986976
		36	LSTM	0.187551	0.433071	0.272055	0.985779
		36	**CNN**	**0.168677**	**0.410703**	**0.230897**	**0.987210**
Badulla	Short-term - One Day (12 lags)	12	RF	0.215237	0.463936	0.260853	0.981941
		12	XGB	0.210603	0.458915	0.262032	0.982330
		12	FNN	0.195593	0.442259	0.260848	0.983589
		12	LSTM	0.215326	0.464033	0.294356	0.981933
		12	CNN	0.196666	0.443470	0.257653	0.983499
	Medium-term - Two Day (24 lags)	24	RF	0.236748	0.486567	0.273748	0.980137
		24	XGB	0.214459	0.463097	0.260429	0.982007
		24	FNN	0.197345	0.444235	0.269845	0.983443
		24	LSTM	0.221745	0.470899	0.297127	0.981396
		24	CNN	0.196579	0.443373	0.261764	0.983507
	Long-term - Three Day (36 lags)	36	RF	0.245633	0.495614	0.279034	0.979398
		36	XGB	0.214446	0.463084	0.263100	0.982014
		36	**FNN**	**0.192443**	**0.438684**	**0.262663**	**0.983859**
		36	LSTM	0.228093	0.477591	0.306606	0.980869
		36	CNN	0.212737	0.461235	0.280405	0.982157
Jaffna	Short-term - One Day (12 lags)	12	RF	0.2152	0.4639	0.2609	0.9819
		12	XGB	0.2106	0.4589	0.2620	0.9823
		12	FNN	0.1956	0.4423	0.2608	0.9836
		12	LSTM	0.2153	0.4640	0.2944	0.9819
		12	CNN	0.1967	0.4435	0.2577	0.9835
	Medium-term - Two Day (24 lags)	24	RF	0.2367	0.4866	0.2737	0.9801
		24	XGB	0.2145	0.4631	0.2604	0.9820
		24	FNN	0.1973	0.4442	0.2698	0.9834
		24	LSTM	0.2217	0.4709	0.2971	0.9814
		24	CNN	0.1966	0.4434	0.2618	0.9835
	Long-term - Three Day (36 lags)	36	RF	0.2456	0.4956	0.2790	0.9794
		36	XGB	0.2144	0.4631	0.2631	0.9820
		36	**FNN**	**0.1924**	**0.4387**	**0.2627**	**0.9839**
		36	LSTM	0.2281	0.4776	0.3066	0.9809
		36	CNN	0.2127	0.4612	0.2804	0.9822

Table 6. Optimal standalone models and hyperparameter configurations for each District

District	Optimal Model	Best Parameters
Colombo	CNN	Long-term - Three Day (36 lags) {'filters': 32, 'kernel_size': 3, 'lr': 0.0015930522616241021, 'batch_size': 16, 'epochs': 30}
Jaffna	FNN	Long-term - Three Day (36 lags) {'n_layers': 1, 'units_l0': 96, 'activation': 'relu', 'alpha': 0.00869299151113955}
Badulla	FNN	Long-term - Three Day (36 lags) {'n_layers': 1, 'units_l0': 64, 'activation': 'relu', 'alpha': 0.0003823475224675188}

5.5. Hybrid Forecasting Performance

To further improve forecasting accuracy, a residual-correction hybrid framework was developed using the best standalone models identified in Section 5.4. In this framework, the selected standalone model first generates the primary UVI forecast. The residual errors produced by the primary model are then treated as a secondary prediction target and modeled using an additional machine learning algorithm. The final forecast is obtained by combining the primary prediction with the estimated residual correction. This strategy enables the hybrid model to capture systematic patterns that remain unexplained by the primary forecasting model and has been successfully applied in various environmental forecasting applications [34]–[37]. For each district, two residual-correction strategies were evaluated using Random Forest (RF) and Extreme Gradient Boosting (XGBoost), respectively. The standalone model is included as a reference baseline to quantify the contribution of the residual-correction stage. The resulting forecasting performance is summarized in Table 7.

Table 7. Hybrid model performance across climatic zones

District	Primary Model	Residual Correction Model	MSE	RMSE	MAE	R^2
Colombo	CNN	–	0.1687	0.4107	0.2309	0.9872
Colombo	CNN	RF	0.1573	0.3967	0.2163	0.9881
Colombo	CNN	XGBoost	0.1592	0.3990	0.2257	0.9879
Badulla	FNN	–	0.1924	0.4387	0.2627	0.9839
Badulla	FNN	RF	0.1819	0.4265	0.2453	0.9847
Badulla	FNN	XGBoost	0.1882	0.4338	0.2557	0.9842
Jaffna	FNN	–	0.1924	0.4387	0.2627	0.9839
Jaffna	FNN	RF	0.1841	0.4291	0.2518	0.9844
Jaffna	FNN	XGBoost	0.1862	0.4315	0.2614	0.9838

The optimal hyperparameter configurations of the primary and residual-correction models are reported in Table 6.

The results indicate that residual-correction hybridization consistently improved forecasting performance relative to the corresponding standalone models. For Colombo, the CNN-RF hybrid achieved the best overall performance, reducing the RMSE from 0.4107 to 0.3967 and increasing the coefficient of determination from 0.9872 to 0.9881. Similar improvements were observed in Badulla and Jaffna, where the FNN-RF hybrid models produced the lowest forecasting errors among all evaluated configurations.

An important observation is that RF-based residual correction consistently outperformed XGBoost-based residual correction across all climatic zones. This finding suggests that Random Forest was more effective in capturing the remaining nonlinear structures embedded within the residual series generated by the primary forecasting models. Overall, the results demonstrate that residual-correction hybridization provides a consistent and measurable improvement in forecasting accuracy beyond that achieved by standalone ML and DL models.

5.6. Diebold–Mariano Statistical Comparison

Although the hybrid models generally produced similar performance levels, formal statistical testing was conducted to determine whether the observed differences in forecasting accuracy were statistically significant. Pairwise comparisons were performed using the Diebold–Mariano (DM) test [38], with squared-error loss and a one-step-ahead forecasting horizon (h = 1). Statistical significance was evaluated at α = 0.05.

Table 8. Diebold–Mariano test results (p-values)

District	Model Comparison	p-value	Decision (α = 0.05)	Better Model
Colombo	CNN-RF vs CNN-XGB	0.0248	Reject H_0	CNN-RF
Badulla	FNN-RF vs FNN-XGB	< 0.001	Reject H_0	FNN-RF
Jaffna	FNN-RF vs FNN-XGB	< 0.001	Reject H_0	FNN-RF

The DM test results indicate that the best-performing RF-based hybrid models were statistically superior to their corresponding XGBoost-based alternatives in all three districts. For Colombo, the comparison between CNN-RF and CNN-XGB yielded a statistically significant result (p = 0.0248), indicating that CNN-RF provided superior predictive accuracy. Similar conclusions were obtained for Badulla and Jaffna, where FNN-RF significantly outperformed FNN-XGB (p < 0.001).

These findings strengthen the conclusions drawn from the error metrics presented in Table 7 by demonstrating that the observed performance improvements are not merely numerical differences but are statistically significant. Consequently, CNN-RF was selected as the final forecasting model for Colombo, while FNN-RF was selected for both Badulla and Jaffna.

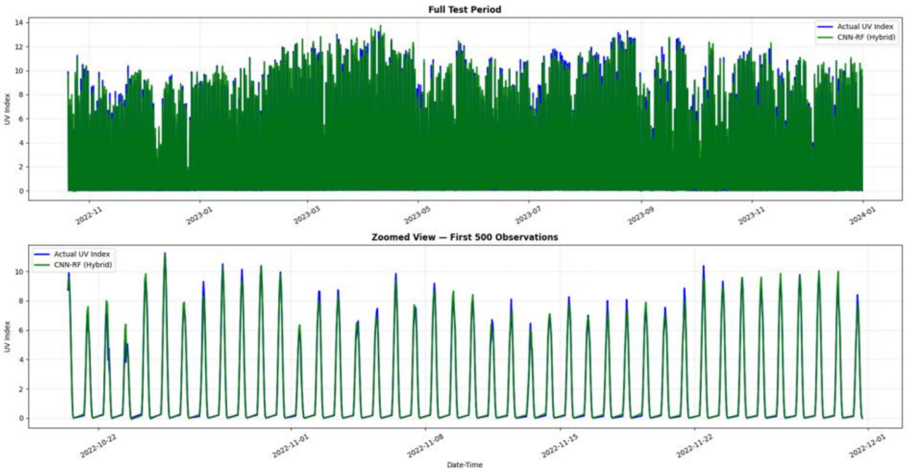

Figure 6. Actual and Predicted UVI Values Generated by the CNN-RF Hybrid Model for Colombo

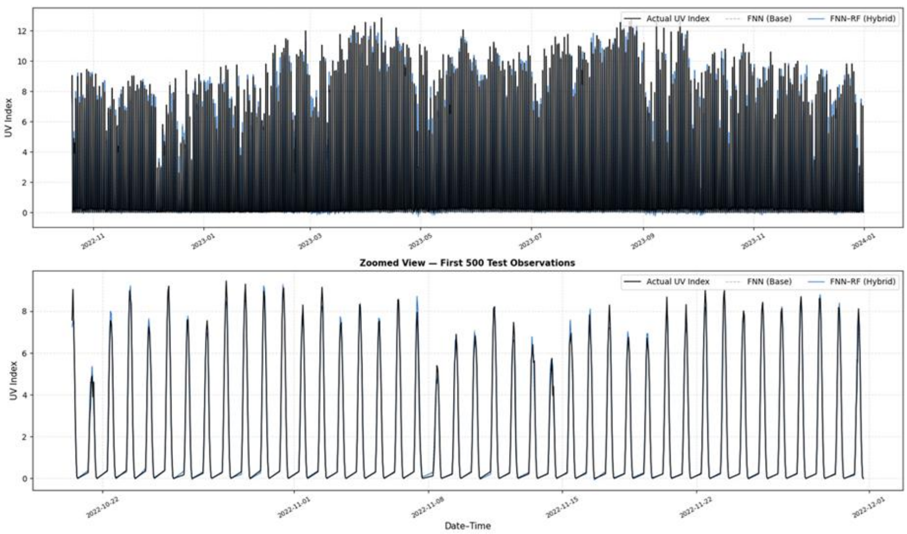

Figure 7. Actual and Predicted UVI Values Generated by the FNN-RF Hybrid Model for Badulla

Figure 6 shows that the CNN-RF model successfully captures the temporal variability of the observed UVI series, with predicted values closely following the actual observations across the evaluation period. The results for Badulla (Figure 7) further demonstrate the ability of the hybrid framework to reproduce both short-term fluctuations and broader temporal trends in hourly UVI observations.

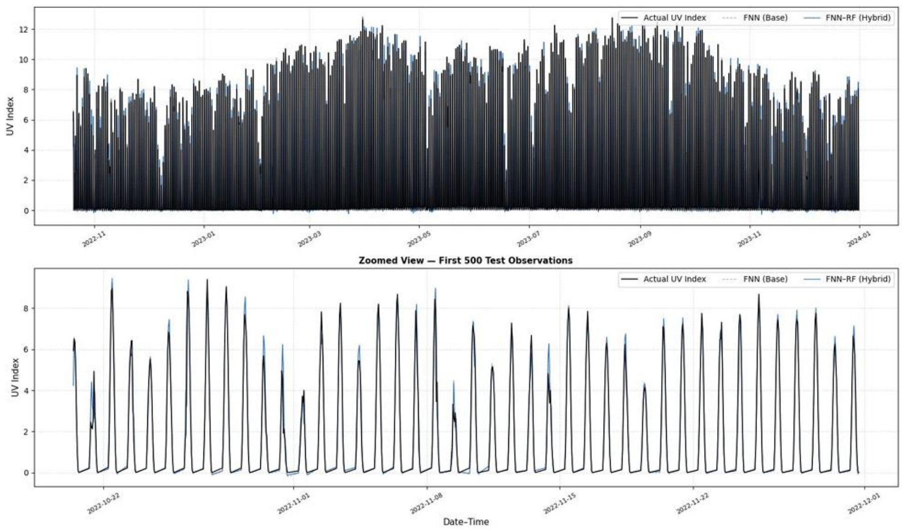

Figure 8. Actual and Predicted UVI Values Generated by the FNN-RF Hybrid Model for Jaffna

A similar pattern is observed for Jaffna, where the FNN-RF model closely tracks the observed UVI dynamics and maintains low prediction errors throughout the testing period.

6. Discussion

This study evaluated traditional statistical, machine learning, deep learning, and residual-correction hybrid approaches for one-hour-ahead UVI forecasting across three climatically distinct regions of Sri Lanka. The results consistently demonstrate that nonlinear forecasting models are better suited for capturing the complex temporal behavior of UVI than conventional linear time-series approaches. More importantly, the improvements achieved through residual-correction hybridization indicate that meaningful predictive information remains embedded within forecast residuals even after standalone model optimization. These findings highlight the value of combining complementary forecasting paradigms to improve short-term environmental prediction.

Another important outcome of this study is the comparison between fixed-lag and varying-lag feature engineering strategies. While the fixed-lag approach provides a standardized representation that facilitates direct comparison across climatic zones, the varying-lag approach allows the input structure to adapt to local temporal dependencies. The superior performance achieved by longer lag windows suggests that UVI dynamics are influenced not only by recent observations but also by recurring daily and multi-day patterns associated with solar radiation processes. Consequently, incorporating broader temporal context appears to be an important factor in improving forecasting accuracy across different climatic conditions.

6.1. Performance of Traditional Statistical Models

The ARIMA benchmark exhibited substantially lower forecasting performance than the ML and DL models across all districts. This outcome is consistent with the well-established limitations of linear statistical models when applied to environmental time series characterized by strong nonlinearity, periodicity, and rapidly changing dynamics [4], [39]. Although ARIMA can effectively capture short-term linear dependencies, its underlying assumptions make it less capable of representing the complex interactions that govern hourly UVI variability.

The observed limitations are likely related to the pronounced diurnal cycle of solar radiation and the influence of local atmospheric processes, which introduce nonlinear relationships that cannot be adequately modeled through linear autoregressive and moving-average components alone [4], [36]. Similar findings have been reported in solar radiation and environmental forecasting studies, where traditional statistical approaches generally serve as useful baseline references but are often outperformed by nonlinear learning algorithms [13], [22]. It should be noted that this study only considered conventional ARIMA models as statistical benchmarks. More advanced seasonal formulations, such as SARIMA, may offer additional capability for capturing recurring temporal patterns and should be considered in future research. Evaluating such models would provide a more comprehensive assessment of statistical forecasting approaches for UVI prediction.

6.2. Performance of Machine Learning and Deep Learning Models

The superior performance of ML and DL models confirms the importance of nonlinear modeling for short-term UVI forecasting. However, forecasting performance was not uniform across climatic zones, suggesting that the effectiveness of a particular architecture depends on local environmental variability and the underlying structure of the UVI series. For Colombo, the CNN architecture achieved the strongest standalone performance. One possible explanation is that the wet-zone climate is characterized by greater atmospheric variability and more frequent cloud-related fluctuations, creating localized temporal patterns that can be effectively captured by convolutional filters. Previous studies in solar irradiance forecasting have similarly shown that CNN-based architectures are particularly effective in environments where short-term variability plays an important role in shaping temporal dynamics [22], [40].

In contrast, FNN models produced the best standalone results in both Badulla and Jaffna. Compared with Colombo, these regions generally exhibit more stable solar radiation conditions and lower short-term variability, allowing simpler feedforward architectures to capture the dominant temporal relationships without requiring more sophisticated feature extraction mechanisms [13], [17]. Taken together, these findings suggest that the suitability of a forecasting architecture is influenced not only by model complexity but also by the characteristics of the underlying climatic environment.

6.3. Implications of Lag-Window Selection

The lag-window analysis revealed that forecasting performance generally improved as longer temporal histories were incorporated into the input feature set. This finding supports the hypothesis that UVI dynamics contain information extending beyond the most recent observations and that effective forecasting requires consideration of recurring temporal structures. The feature selection analysis consistently identified lag 1, lags 11–13, lag 24, and lag 36 as highly informative predictors across all districts. These lag positions correspond closely to recurring daily and multi-day solar radiation cycles, indicating that hourly UVI behavior is strongly influenced by periodic temporal patterns [7], [8]. The consistency of this lag structure across wet, intermediate, and dry climatic zones suggests that certain temporal dependencies remain stable despite regional climatic differences.

From a practical perspective, these results emphasize the importance of feature engineering in environmental forecasting applications. Rather than relying exclusively on recent observations, incorporating temporally meaningful lag structures can substantially improve predictive performance while maintaining relatively simple model architectures. This finding may be particularly valuable for data-sparse regions where forecasting systems must be developed using limited input variables.

6.4. Implications of the Residual-Correction Hybrid Framework

One of the most important findings of this study is the consistent improvement achieved through residual-correction hybridization. By treating the prediction errors of the best-performing standalone model as a secondary forecasting target, the hybrid framework is able to capture structured information that remains unexplained after the initial prediction stage. Similar error-correction strategies have been successfully applied in other environmental forecasting domains, including photovoltaic power forecasting and solar radiation prediction [23], [34]–[36].

The observed improvements across all climatic zones suggest that standalone models, despite their strong predictive performance, do not fully exploit all information contained within the UVI time series. Residual modeling therefore provides an additional learning stage capable of extracting predictive signals that remain embedded in forecast errors. This finding supports the broader view that combining complementary forecasting models can improve predictive performance beyond what is achievable using a single forecasting architecture alone.

An additional observation is the consistent superiority of RF-based residual correction over XGBoost-based residual correction. A plausible explanation is that the ensemble averaging mechanism of Random Forest is particularly effective at modeling low-amplitude residual patterns while maintaining robustness against overfitting [37], [41]. In contrast, boosting-based approaches iteratively focus on correcting previous errors, which may offer less advantage when the residual series already contains relatively small and irregular prediction errors. Although further investigation is required to confirm the underlying mechanisms, the results indicate that Random Forest constitutes an effective residual-learning component for short-term UVI forecasting.

6.5. Statistical Validation and Model Robustness

The Diebold–Mariano test provided additional evidence that the forecasting improvements achieved by the selected hybrid models were statistically meaningful rather than arising from random variation [39]. The rejection of the null hypothesis of equal predictive accuracy across all districts indicates that the performance differences observed among the competing hybrid models are unlikely to be attributable to chance alone. Consequently, the statistical analysis reinforces the reliability of the selected CNN-RF and FNN-RF forecasting frameworks.

The use of statistical significance testing is particularly important in forecasting studies because small numerical differences in error metrics do not necessarily imply meaningful performance improvements. By complementing conventional error measures with formal hypothesis testing, the study provides stronger evidence regarding the comparative effectiveness of the evaluated forecasting strategies. Similar applications of the Diebold–Mariano test have become increasingly common in environmental and atmospheric forecasting research [37], [38], [42].

It should be noted that model evaluation was ultimately performed using an independent hold-out test set, while TimeSeriesSplit cross-validation was employed during hyperparameter optimization. Although this approach reflects realistic forecasting conditions and minimizes information leakage, future studies may further strengthen robustness assessments through rolling-origin evaluation or nested time-series cross-validation frameworks.

6.6. Climatic-Zone-Specific Forecasting Behavior

The results also reveal meaningful differences in forecasting behavior across Sri Lanka's climatic zones. Colombo, representing the wet zone, exhibited slightly greater forecasting difficulty during the standalone modeling stage. One possible explanation is the higher atmospheric variability associated with cloud formation and humidity in coastal tropical environments, which can introduce additional short-term fluctuations in surface UV radiation [26], [33]. Such variability may reduce the predictability of UVI when forecasts are based solely on historical observations.

Badulla and Jaffna exhibited different forecasting characteristics despite achieving comparable overall performance. The relatively strong results obtained in Badulla may be associated with more stable temporal patterns arising from its intermediate climatic conditions. In contrast, forecasting performance in Jaffna suggests that factors beyond simple cloud variability may contribute to local UVI dynamics [27], [43]. Previous studies have reported that aerosol loading, marine influences, and other atmospheric processes can affect UV transmission in coastal environments, potentially introducing variability that is difficult to infer solely from historical UVI values [27], [43]. These findings highlight that forecasting performance is influenced not only by model architecture but also by the environmental characteristics of the target region. Consequently, forecasting frameworks that perform optimally in one climatic setting may not necessarily represent the best solution for another, even within the same country.

6.7. UVI Trends and Public Health Implications

The exploratory analysis revealed consistently elevated UVI levels during 2023 relative to previous years across all three districts. Although the present study does not attempt to attribute the causes of this increase, the observed pattern is broadly consistent with reports indicating that surface UV radiation can be influenced by changes in cloud cover, aerosol concentrations, and atmospheric composition [28], [40], [43].

From a practical perspective, the prevalence of high and very high UVI conditions across all climatic zones underscores the importance of continuous monitoring and reliable short-term forecasting. Accurate UVI forecasts can support early-warning systems, improve public awareness of harmful UV exposure, and assist individuals and public health agencies in implementing preventive measures [4]–[6], [9], [35], [36].

More broadly, the results demonstrate the potential of data-driven forecasting approaches to support environmental risk management in tropical regions where ground-based monitoring infrastructure may be limited. By providing accurate short-term predictions using publicly available satellite-derived observations, the proposed framework offers a practical pathway toward operational UVI forecasting and climate-adaptation planning in data-sparse environments.

7. Conclusions

This study developed and evaluated a residual-correction hybrid framework for one-hour-ahead UVI forecasting across three climatically distinct regions of Sri Lanka using hourly NASA Power observations. The proposed framework systematically compared traditional statistical, machine learning, deep learning, and hybrid forecasting approaches under a consistent experimental setting. The results demonstrate that nonlinear learning-based methods substantially outperform conventional statistical forecasting models for hourly UVI prediction. Across all climatic zones, hybrid residual-correction models consistently achieved the highest predictive accuracy, indicating that additional predictive information remained embedded within the residual errors of the standalone models. The findings further highlight the importance of feature engineering, as forecasting performance improved when longer temporal dependencies were incorporated into the input representation.

Beyond predictive performance, this study provides evidence that residual-correction hybridization constitutes an effective strategy for environmental time-series forecasting in climatically heterogeneous regions. The results also suggest that optimal forecasting architectures may vary across climatic zones, emphasizing the importance of considering local environmental characteristics when designing forecasting systems. Because the framework relies exclusively on publicly available satellite-derived observations, it offers a practical solution for operational UVI forecasting in data-sparse tropical regions. Several limitations should be acknowledged. First, the study adopted a univariate forecasting framework based solely on historical UVI observations. Second, model evaluation was performed using a single hold-out test period, although time-series cross-validation was employed during hyperparameter optimization. Third, only one-hour-ahead forecasting was considered, and seasonal statistical benchmarks such as SARIMA were not evaluated.

Future research should investigate multivariate forecasting frameworks incorporating meteorological and atmospheric variables, including cloud optical depth, total column ozone, aerosol optical depth, and temperature. Additional work should also explore multi-step forecasting horizons, more advanced statistical benchmarks, explainable artificial intelligence techniques, and real-time deployment scenarios to further support public health decision-making and UV early-warning systems.

Author Contributions: Conceptualization: H.N.K.; Methodology: H.N.K.; Software: H.N.K. and K.G.A.Y.; Validation: H.N.K. and K.G.A.Y.; Formal analysis: H.N.K. and K.G.A.Y.; Investigation: H.N.K. and K.G.A.Y.; Resources: S.M.A.; Data curation: H.N.K.; Writing—original draft preparation: H.N.K.; Writing—review and editing: K.G.A.Y., S.M.A., and C.L.I.S.F.; Visualization: H.N.K.; Supervision: S.M.A. and C.L.I.S.F.; Project administration: H.N.K., S.M.A., and C.L.I.S.F. All authors have read and agreed to the published version of the manuscript.

Funding: This research received no external funding.

Data Availability Statement: The datasets and source code used in this study, including data acquisition, preprocessing, feature engineering, model development, and evaluation scripts, are publicly available at. https://github.com/HiruNavodya/Ultraviolet-index-analysis-and-forecasting .The repository also contains documentation describing the NASA POWER data retrieval process and the corresponding analysis workflow.

Acknowledgments: The authors used AI-based writing assistance tools to improve the clarity and grammatical quality of this manuscript. All scientific content, data analysis, interpretations, and conclusions remain solely the work of the authors.

Conflicts of Interest: The authors declare no conflict of interest

References

[1] X. Tang, T. Yang, D. Yu, H. Xiong, and S. Zhang, "Current insights and future perspectives of ultraviolet radiation (UV) exposure: Friends and foes to the skin and beyond the skin," *Environ. Int.*, vol. 185, p. 108535, Mar. 2024, doi: 10.1016/j.envint.2024.108535.

[2] O. Langselius *et al.*, "Global burden of cutaneous melanoma incidence attributable to ultraviolet radiation in 2022," *Int. J. Cancer*, vol. 157, no. 6, pp. 1110–1119, Sep. 2025, doi: 10.1002/ijc.35463.

[3] A. Brozyna, B. Zbytek, J. Granese, J. A. Carlson, J. Ross, and A. Slominski, "Mechanism of UV-related carcinogenesis and its contribution to nevi/melanoma," *Expert Rev. Dermatol.*, vol. 2, no. 4, pp. 451–469, Aug. 2007, doi: 10.1586/17469872.2.4.451.

[4] World Health Organization, "Radiation: The Known Health Effects of Ultraviolet Radiation," *World Health Organization*, 2024. https://www.who.int/news-room/questions-and-answers/item/radiation-the-known-health-effects-of-ultraviolet-radiation (accessed Apr. 04, 2026).

[5] World Health Organization, "Global Solar UV Index: A Practical Guide," *World Health Organization*, 2002. https://www.who.int/publications/i/item/9241590076 (accessed Apr. 04, 2026).

[6] C. J. Heckman, K. Liang, and M. Riley, "Awareness, understanding, use, and impact of the UV index: A systematic review of over two decades of international research," *Prev. Med. (Baltim).*, vol. 123, pp. 71–83, Jun. 2019, doi: 10.1016/j.ypmed.2019.03.004.

[7] V. Fioletov, J. B. Kerr, and A. Fergusson, "The UV Index: Definition, Distribution and Factors Affecting It," *Can. J. Public Heal.*, vol. 101, no. 4, pp. I5–I9, Jul. 2010, doi: 10.1007/BF03405303.

[8] B. L. Diffey, "Solar ultraviolet radiation effects on biological systems," *Phys. Med. Biol.*, vol. 36, no. 3, pp. 299–328, Mar. 1991, doi: 10.1088/0031-9155/36/3/001.

[9] U.S. Environmental Protection Agency, "UV Index Overview," *U.S. Environmental Protection Agency*, 2026. https://www.epa.gov/enviro/uv-index-overview (accessed Apr. 04, 2026).

[10] K. Fragkos *et al.*, "Twenty-Year Climatology of Solar UV and PAR in Cyprus: Integrating Satellite Earth Observations with Radiative Transfer Modeling," *Remote Sens.*, vol. 16, no. 11, p. 1878, May 2024, doi: 10.3390/rs16111878.

[11] S. Madronich, "The Atmosphere and UV-B Radiation at Ground Level," in *Environmental UV Photobiology*, Boston, MA: Springer US, 1993, pp. 1–39. doi: 10.1007/978-1-4899-2406-3_1.

[12] L. González-Rodríguez *et al.*, "Ultraviolet erythemal radiation in Central Chile: direct and indirect implication for public health," *Air Qual. Atmos. Heal.*, vol. 14, no. 10, pp. 1533–1548, Oct. 2021, doi: 10.1007/s11869-021-01037-3.

[13] C. Voyant *et al.*, "Machine learning methods for solar radiation forecasting: A review," *Renew. Energy*, vol. 105, pp. 569–582, May 2017, doi: 10.1016/j.renene.2016.12.095.

[14] K. P. Arandara, R. A. Attalage, and M. T. R. Jayasinghe, "Thermal Comfort with Evaporative Cooling for Tropical Climates," in *Proc. Int. Conf. Sustainable Built Environment (ICSBE-2010)*, 2010. [Online]. Available: http://www.civil.mrt.ac.lk/web/conference/ICSBE_2010/vol_01/51.pdf

[15] B. Mayer and A. Kylling, "Technical note: The libRadtran software package for radiative transfer calculations - description and examples of use," *Atmos. Chem. Phys.*, vol. 5, no. 7, pp. 1855–1877, Jul. 2005, doi: 10.5194/acp-5-1855-2005.

[16] A. Chatzopoulou, K. Tourpali, A. F. Bais, and P. Braesicke, "21st century surface UV radiation changes deduced from CMIP6 models: part I—evolution of major influencing factors," *Photochem. Photobiol. Sci.*, vol. 24, no. 1, pp. 89–109, Jan. 2025, doi: 10.1007/s43630-024-00675-7.

[17] S. V. D, T. S. V S, and M. Meleet, "Ultraviolet index analysis and forecasting using deep learning methodologies for Bengaluru city," *EPRA Int. J. Multidiscip. Res.*, vol. 8, no. 7, 2022, [Online]. Available: https://eprajournals.com/IJMR/article/7361

[18] S. S. Prasad, R. C. Deo, S. Salcedo-Sanz, N. J. Downs, D. Casillas-Pérez, and A. V. Parisi, "Enhanced joint hybrid deep neural network explainable artificial intelligence model for 1-hr ahead solar ultraviolet index prediction," *Comput. Methods Programs Biomed.*, vol. 241, p. 107737, Nov. 2023, doi: 10.1016/j.cmpb.2023.107737.

[19] A. A. M. Ahmed, M. H. Ahmed, S. K. Saha, O. Ahmed, and A. Sutradhar, "Optimization algorithms as training approach with hybrid deep learning methods to develop an ultraviolet index forecasting model," *Stoch. Environ. Res. Risk Assess.*, vol. 36, no. 10, pp. 3011–3039, Oct. 2022, doi: 10.1007/s00477-022-02177-3.

[20] A. S. Syahab, G. L. Pamungkas, and S. Akmal, "The Classification of Ultraviolet Index Using Logistic Regression and Random Forest methods for Predicting Extreme Conditions," in *Advances in Intelligent Systems Research*, 2024, pp. 4–14. doi: 10.2991/978-94-6463-366-5_2.

[21] E. Ervianto *et al.*, "Assessing the Efficacy of the UV Index in Predicting Surface UV Radiation: A Comprehensive Analysis Using Statistical and Machine Learning Methods," *Indones. Rev. Phys.*, vol. 6, no. 2, pp. 99–121, Dec. 2023, doi: 10.12928/irip.v6i2.8216.

[22] H. Zang, L. Liu, L. Sun, L. Cheng, Z. Wei, and G. Sun, "Short-term global horizontal irradiance forecasting based on a hybrid CNN-LSTM model with spatiotemporal correlations," *Renew. Energy*, vol. 160, pp. 26–41, Nov. 2020, doi: 10.1016/j.renene.2020.05.150.

[23] R. Zhang *et al.*, "A hybrid deep learning model with error correction for photovoltaic power forecasting," *Front. Energy Res.*, vol. 10, Aug. 2022, doi: 10.3389/fenrg.2022.948308.

[24] A. Taha, P. Makeen, and N. Nazih, "Short-term and long-term solar irradiance forecasting with advanced machine learning techniques in Zafarana, Egypt," *Sci. Rep.*, vol. 15, no. 1, p. 39553, Nov. 2025, doi: 10.1038/s41598-025-24853-4.

[25] A. Taha, N. Nazih, and P. Makeen, "Wind speed prediction based on variational mode decomposition and advanced machine learning models in zaafarana, Egypt," *Sci. Rep.*, vol. 15, no. 1, p. 15599, May 2025, doi: 10.1038/s41598-025-98543-6.

[26] I. G. N. P. Dharmayasa, C. A. Simatupang, and D. M. Sinaga, "NASA Power's: an alternative rainfall data resources for hydrology research and planning activities in Bali Island, Indonesia," *J. Infrastruct. Plan. Eng.*, vol. 1, no. 1, pp. 1–7, Apr. 2022, doi: 10.22225/jipe.1.1.2022.1-7.

[27] H. Kadhim Tayyeh and R. Mohammed, "Analysis of NASA POWER reanalysis products to predict temperature and precipitation in Euphrates River basin," *J. Hydrol.*, vol. 619, p. 129327, Apr. 2023, doi: 10.1016/j.jhydrol.2023.129327.

[28] G. C. Rodrigues and R. P. Braga, "Evaluation of NASA POWER Reanalysis Products to Estimate Daily Weather Variables in a Hot Summer Mediterranean Climate," *Agronomy*, vol. 11, no. 6, p. 1207, Jun. 2021, doi: 10.3390/agronomy11061207.

[29] J. A. Ingio, A. S. Nsang, and A. Iorliam, "Optimizing Rice Production Forecasting Through Integrating Multiple Linear Regression with Recursive Feature Elimination," *J. Futur. Artif. Intell. Technol.*, vol. 1, no. 2, pp. 96–108, Aug. 2024, doi: 10.62411/faith.2024-17.

[30] W. Aprianti and I. Mukhlash, "Handling Missing Value on Meteorological Data Classification with Rough Set Based Algorithm," *Glob. J. Pure Appl. Math.*, vol. 11, no. 3, pp. 1147–1155, 2015, [Online]. Available: https://www.ripublication.com/gjpam 2015/gjpamv11n3_01.pdf

[31] M. Hasanpour Kashani and Y. Dinpashoh, "Evaluation of efficiency of different estimation methods for missing climatological data," *Stoch. Environ. Res. Risk Assess.*, vol. 26, no. 1, pp. 59–71, Jan. 2012, doi: 10.1007/s00477-011-0536-y.

[32] International Commision on Non-Ionizing Radiation Protection, "UV Index: Global Solar Ultraviolet Index (UVI)," *ICNIRP*. https://www.icnirp.org/en/applications/uv-index/index.html

[33] World Health Organization, "Radiation: The Ultraviolet (UV) Index," *World Health Organization*, 2022. https://www.who.int/news-room/questions-and-answers/item/radiation-the-ultraviolet-(uv)-index

[34] M. D. Teja and G. M. Rayalu, "Hybrid time series and machine learning models for forecasting cardiovascular mortality in India: an age specific analysis," *BMC Public Health*, vol. 25, no. 1, p. 2150, Jun. 2025, doi: 10.1186/s12889-025-23318-7.

[35] S. Bhuvaneshwari and S. N. S. Rajini, "A Novel Hybrid Model for Stock Price Forecasting: Combining ARIMA, Random Forests, and Gradient Boosting Techniques," *Libr. Prog. Int.*, vol. 44, no. 2s, 2024, doi: 10.48165/bapas.2024.44.2.1.

[36] G. P. Zhang, "Time series forecasting using a hybrid ARIMA and neural network model," *Neurocomputing*, vol. 50, pp. 159–175, Jan. 2003, doi: 10.1016/S0925-2312(01)00702-0.

[37] L. B. Sina, C. A. Secco, M. Blazevic, and K. Nazemi, "Hybrid Forecasting Methods—A Systematic Review," *Electronics*, vol. 12, no. 9, p. 2019, Apr. 2023, doi: 10.3390/electronics12092019.

[38] G. H. Bernhard, A. F. Bais, P. J. Aucamp, A. R. Klekociuk, J. B. Liley, and R. L. McKenzie, "Stratospheric ozone, UV radiation, and climate interactions," *Photochem. Photobiol. Sci.*, vol. 22, no. 5, pp. 937–989, Apr. 2023, doi: 10.1007/s43630-023-00371-y.

[39] F. X. Diebold and R. S. Mariano, "Comparing Predictive Accuracy," *J. Bus. Econ. Stat.*, vol. 13, no. 3, pp. 253–263, Jul. 1995, doi: 10.1080/07350015.1995.10524599.

[40] P. J. Neale *et al.*, "Environmental consequences of interacting effects of changes in stratospheric ozone, ultraviolet radiation, and climate: UNEP Environmental Effects Assessment Panel, Update 2024," *Photochem. Photobiol. Sci.*, vol. 24, no. 3, pp. 357–392, Mar. 2025, doi: 10.1007/s43630-025-00687-x.

[41] B. Ladjal *et al.*, "Hybrid deep learning CNN-LSTM model for forecasting direct normal irradiance: a study on solar potential in Ghardaia, Algeria," *Sci. Rep.*, vol. 15, no. 1, p. 15404, May 2025, doi: 10.1038/s41598-025-94239-z.

[42] A. Chatzopoulou, K. Tourpali, A. F. Bais, and P. Braesicke, "Effects of different aerosol types on surface UV radiation in the 21st century," *Atmos. Environ.*, vol. 362, p. 121595, Dec. 2025, doi: 10.1016/j.atmosenv.2025.121595.

[43] P. Kumari and D. Toshniwal, "Deep learning models for solar irradiance forecasting: A comprehensive review," *J. Clean. Prod.*, vol. 318, p. 128566, Oct. 2021, doi: 10.1016/j.jclepro.2021.128566.